Resonant spatial tracking using nanostructured Resonant Waveguide Grating for multispectral sensing by imaging

Kristelle Bougot-Robin, W. Cao, Shunbo Li, H. Benisty, Weijia Wen

Resonant spatial tracking using nanostructured Resonant Waveguide Grating for multispectral sensing by imaging

Kristelle Bougot-Robin[a,d,*], Wenbin Cao[b], Shunbo Li[b], Henri Benisty[c], Weijia Wen[b]
[a]Institute for Advanced Study, Hong Kong University of Science and Technology, Clear Water Bay, Kowloon, Hong Kong, SAR China
[b]Physics Department, Hong Kong University of Science and Technology, Clear Water Bay, Kowloon, Hong Kong, SAR China
[c]Institut Optique Graduate School, CNRS, Université Paris Sud, France
[d]currently at Chemistry department, Imperial College London, United Kingdom

ABSTRACT

Resonant profile shift resulting from a change of resonant conditions is classically used for sensing, either liquid refractive index or immobilized biological layer effective thickness. Resonant waveguide gratings (RWG) allow sensing over a large spectral domain, depending on the materials and geometrical parameters of the grating. Profiles measurements usually involve scanning instrumentation. We recently demonstrated that direct imaging multi-assay RWGs sensing may be rendered more robust using spatial Fano profiles from "chirped" RWG chips. The scheme circumvents the classical but demanding scans: instead of varying angle or wavelength through fragile moving parts or special optics, a RWG structure parameter is varied. Our findings are illustrated with resonance profiles from nanostructured silicon nitride waveguide on glass. A sensitivity down to $\Delta n=2x10^{-5}$ or biomolecules mass density of 10 pg/mm^2 is demonstrated through theory and experiments. To assess different sensing wavelength, the period might also vary within the same chip support. We discuss guiding properties and sensing sensitivities of RWG sensing over the whole visible spectral range. Resonant profiles are analyzed using a correlation approach, correlating the sensed signal to a zero-shifted reference signal. This analysis was demonstrated to be more accurate than usual fitting, for analyzing signals including noise contribution. The current success of surface plasmon imaging suggests that our work could leverage an untapped potential to extend such techniques in a convenient and sturdy optical configuration. Moreover, extended spectral range sensing can be addressed by dielectric waveguide structures. This allows sensitive sensing of small volumes of analyte, which can be circulated close from the resonant waveguide. Together with the demonstration of highly accurate fits through correlation analysis, our scheme based on a "Peak-tracking chip" demonstrates a new technique for multispectral sensitive sensing through nanostructured chip imaging.

Keywords: Resonant sensing, resonant waveguide gratings, multispectral, imaging

1. INTRODUCTION

Label-free optical sensing can be performed thanks to resonant structures, notably by measuring their resonance response through their spectrum. It can be used to perform liquid refractive index sensing or label-free biological sensing, by determining the effective thickness of a biological layer immobilized on the chip surface. Surface plasmon resonance or dielectric resonant structures can be used. Resonant waveguide gratings (RWG) allow sensing over a large spectral domain, easily attained by a combination of available materials and geometrical parameters of the grating.

Change of resonance condition might be measured through the shift of the resonant response, for instance from spectral measurement ($u\equiv\lambda$) [1,2] or angular scan ($u\equiv\theta$) [3], or through the change of diffraction efficiency I_{refl} ($u=u_0$) measured in fixed spectro-angular optical configuration [4]. While the shift in resonance response is a more robust measurement as it is based on an intensity sequence instead of one point, it however relies on costly instrumentation. For

spectral based measurement, sensing in a 2D array format is ensured either using a spectro-imager [2] or tunable light source [1]. As for angular resonance profiles, they are measured by highly precise angular scan [3]. Intensity variation at a single (λ_0,θ_0) condition might also be used, but such single point measurement is more prone to background contribution and therefore less reliable.
To combine simple instrumentation [4] and robust measurement based on near-resonance intensity sequence, we recently proposed a scheme based on engineered spatial intensity sequences [5,6]. Instead of varying a wave parameter through instrumentation, our scheme is based on a specially designed nanostructuration having one of its spatial parameters *u* varied to scan the resonance. The variation profile is then detected on different pixels of an imaging array, forming adequate "tracks". The structure (materials and geometry, including layer thickness and nanostructured patterns) are chosen to perform sensing at a targeted wavelength with a high degree of flexibility in nanostructured pattern on a 2D chip format.

We recently demonstrated that this direct imaging multi-assay RWGs sensing method may be rendered more robust using spatial Fano profiles that naturally arise from "chirped" RWG chips that request relaxed fabrication constraints. Tracks spatial profiles (2D images) have sufficient discretization for sensitive sensing and accurate peak shift tracking. Resonant profiles are analyzed using a correlation approach, correlating the sensed signal to a zero-shifted reference signal.
We first introduce the sensing principle of sensing resonant profiles through imaging varying nanostructuration. We then explain how the nanostructuration can be further exploited, in order to be able to sense several wavelength of the same chip support. Experimental validations are also presented.

2. SENSING PRINCIPLE

2.1 Resonant sensing through imaging

Resonant response depends on layer thicknesses, etching depth, filling factor, layers refractive indexes and period. We call "tracks" the elementary sensing area on the chip [5]. To scan around the resonance, the waveguide structure is varied slowly along a track and a resonant profile can then be extracted from spatial information of a monochromatic picture. In this paper, we illustrate the case of filling factor variation delivering Fano spatial profiles and vary as well the period, to be able to perform sensing of several wavelengths using the same chip support. With tracks elongating along one dimension, and periods varied along the other, the scheme obviously fits with 2D array sensing, as long as the elementary RWGs are imaged on a limited number of pixels of the array.

For sensing in the visible range, we choose silicon nitride RWGs on glass substrate, both materials being transparent over the visible range with n_{SiN}~2, and n_{SiO2}~1.5. Our previous demonstrations were mostly based on monochromatic sensing, with multiple tracks of the same geometry on the same surface. Here, we also vary the track period, so that several wavelengths can be sensed using the same chip support and cover the visible range.

In Fig. 1(A), we give the resonant response for refractive indices of the analyte of n=1.39 and n=1.4, namely for a change $\Delta n=10^{-2}$. The tracks discretization illustrated here corresponds to a wavelength λ=545 nm obtained for a period Λ=450 nm, as will be discussed later. Fig. 1(B) gives the intensity images, as can be measured experimentally using a monochromatic set-up and illuminating the chip in resonant conditions. A scheme of a track is given in Fig. 1(C) and results in a stepwise profile as seen in Fig. 1(A) due to fabrication limitation (the groove width varies by steps of 4 nm, due to fabrication limitation). The elementary RWGs of the tracks are called « micropads », each micropad having its filling factor $f_m=d_m/\Lambda_m$, where m is the index of the micropad, and Δd=4 nm. With a period of Λ=450 nm as illustrated here, it corresponds to Δf=0.0089.

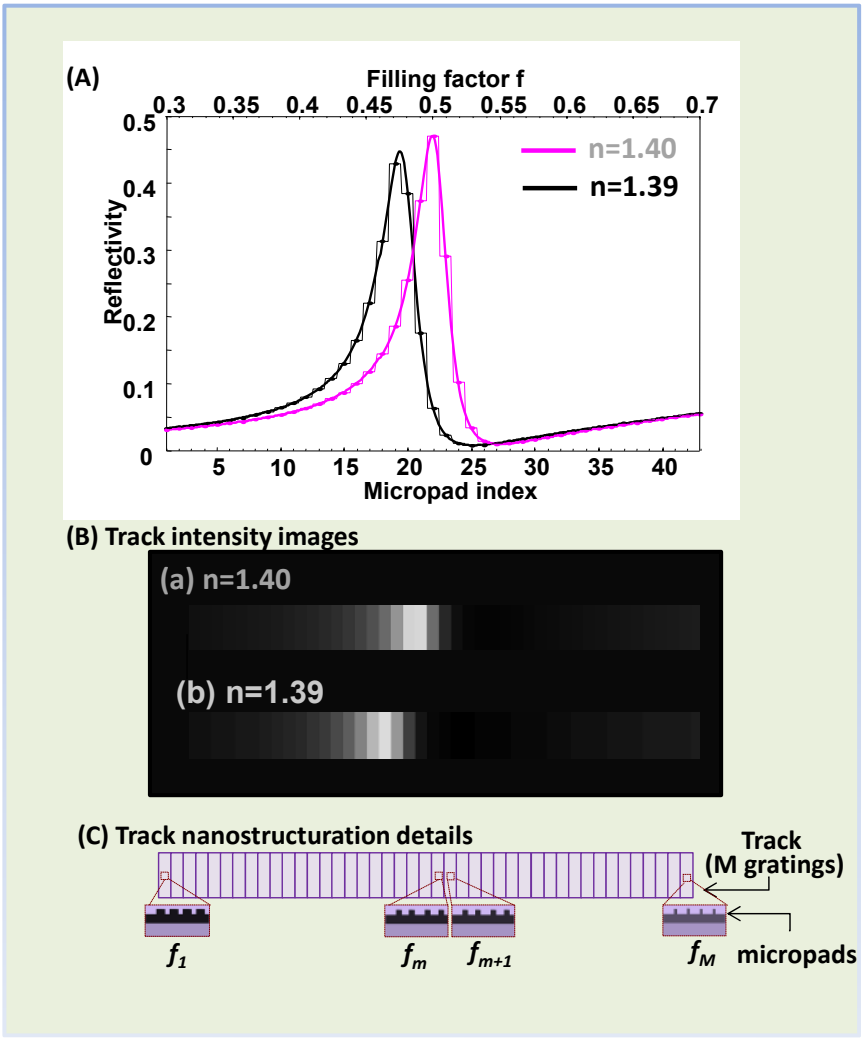

Figure 1: (A) Fano profiles for sensed media of refractive index n_A=1.39 and n_B=1.4 (B) Same as in (A) but in intensity scale, corresponding to measured images on a monochromatic set-up (C) Track details, with micropads of different filling factors, $f_m=d_m/\Lambda$, where d_m is the groove width, increasing along the track, to span from f_1~0.35 and f_M=0.65.

2.2 Multispectral sensing

To assess different wavelengths over the whole visible range, the period can also vary within the same chip support, thus achieving different sensing areas for different wavelengths [8]. Grating realized at periods Λ=380 to Λ =520 nm allow to cover the whole visible range on one cm² chip. We discuss guiding properties and sensing sensitivities of RWG sensing over the whole spectral range, with only geometrical pattern parameters being varied, while layer thicknesses and etching depths are kept constant.

For each of the period, the filling factor is varied on a range of f_1=0.35 to f_M=0.65. The pattern is defined by electron-beam lithography, and the minimal geometrical increase for the groove width is of 4 nm. Therefore, the filling factor variation step between adjacent micropads will decrease from Δf_{380nm} = 0.0105 down to Δf_{520nm} = 0.0077. This results in a smaller number of tracks needed to cover the whole filling factor range with the shortest period than with the largest. A scheme of the nanostructured chip is given in Figure 2(A,B), with (A) side view, with constant thickness of substrate and waveguide thickness and (B) top view, with the varying period to cover the whole visible spectrum and allow sensing accordingly. Several such patterns can be placed on a single chip, therefore allowing multispectral array sensing, or simply using some of the tracks for reference, to correct from drift (mechanical, temperature, etc.)

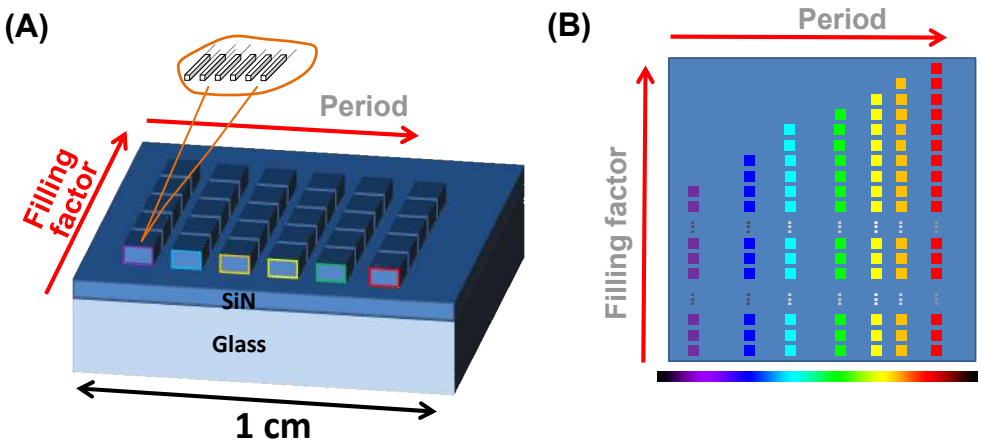

Figure 2: (A) Side view of the chip design, with constant geometrical thickness for the SiN waveguide and same glass substrate. The gratings geometrical parameters are varied in term of period and filling factor and have the same etching depth (B) Top view of the design: the filling factor is varied in the vertical direction to obtain spatial resonant profiles and the period is varied in the horizontal direction, to be able to sense multiple wavelength using the same chip support.

3. NANOSTRUCTURATION FOR MULTISPECTRAL SENSING

Photonic properties of RWGs basically scale as $\Lambda/\lambda \sim 0.83$, and we keep the thickness of the layers and the etching depth of the grating similar for all tracks, with a thickness of 110 nm for the SiN layer, etched over a thickness of 45 nm. Consequently, spectrally the mode will be more confined in the structure of larger wavelength, resulting in a larger Q-factor in term of spectral resonance response.

We calculated the diffraction efficiency depending of the filling factor and refractive index of the analyte using scattering matrix formalism [7]. The resulting diffraction efficient maps are given in Figure 3(A-C) for 3 different wavelength and periods. The chosen wavelength are λ=450 nm with Λ=380 nm, λ=545 nm with Λ=450 nm and λ=630 nm with Λ=520 nm, illustrating sensing over most of the visible range. In Figure 3(D-F), we give the image of a single track for each of the wavelengths, focusing on micropads around resonance. Corresponding Fano response profiles are also given. The diffraction efficiency clearly decreases as the period increases as explained above. In term of filling factor, the range remains the same for the different period, since it scales like Λ/λ.

All spatial profiles have sufficient discretization to properly sample resonances and can be used for accurate sensing. They can be fitted with a correlation approach, specifically for shift determination, as presented in the next section.

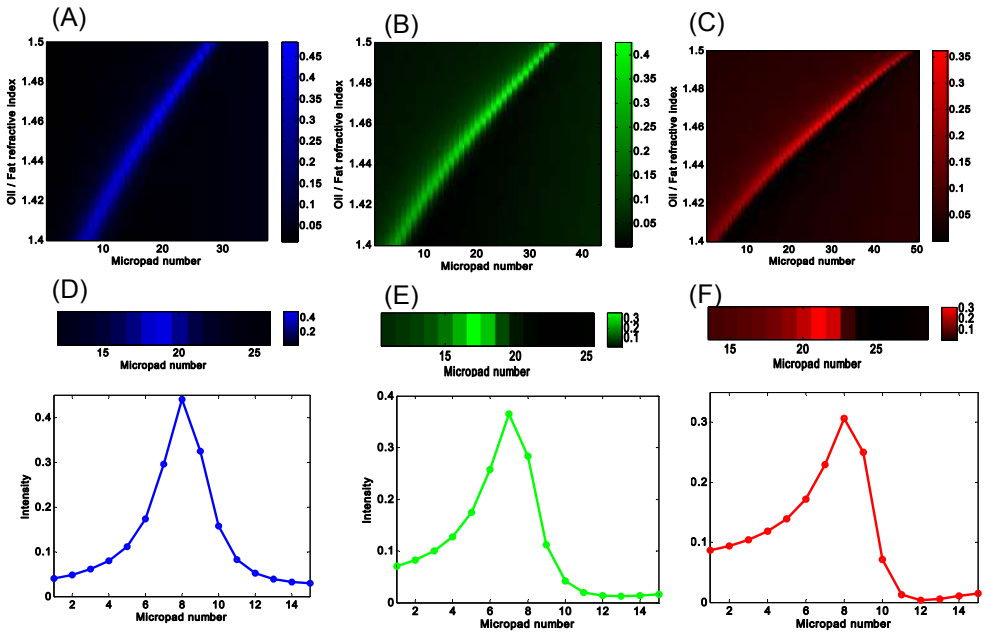

Figure 3: (A-C) Map of monochromatic track images depending on the refractive index of the analyte at the wavelength of (A) λ=480 nm, (B) λ=550 nm and (C) λ=630 nm (D-F) Track images extracted for a given refractive index n=1.45 on a number of 15 micropads, for each of the wavelengths, with their intensity profiles plotted as well.

3.1 Peak shift determination with correlation analysis

For sensing purpose, it is necessary to quantify the shift of the resonant response, and then deduce the change of refractive index (or the amount of biomolecules) at the chip surface.

We demonstrated that correlation analysis was robust to Fano lineshape asymmetry and gave better accuracy than usual fitting models (Gauss and Lorentz fitting model). In Fig.4, we illustrate the shift calculation using correlation analysis.

We call S the signal to analyze and S_{ref} the reference signal. Here the signal images consist in 2D matrix, of dimensions $D_x \times M\ D_y$, where M is the number of micropad per track and D_x and D_y are the number of pixels spanning a micropad in both directions.

Note that the number of pixels in the vertical direction might be D_y=1, and therefore our correlation analysis model can be applied to any Fano-lineshape signal. This shift in micropad unit is considered as proportional to the refractive index change at the chip surface. For a large refractive index span, a curvature is observed and a weakly nonlinear calibration might be necessary to interpret the peak shift.

Except from parasitic contributions the D_x lines ideally have the same signal, and we therefore calculate the correlation on each of the lines between the signal and the reference images and average over the different lines. The difference between the lines may have optical origins (for instance distortion) or be due to fabrication variability. Noise contribution is also different on each of the pixel (i, j).
The correlation function can be expressed as by equation (1) as follows:

$$C(\Delta j) = D_x^{-1} \Sigma_j \Sigma_i \, \bar{S}(i,j) \otimes \bar{S}_{\text{ref}}(i,j) \qquad (1)$$

To increase the precision of this correlation beyond the micropad unit and perform sensitive sensing, meaning have a precise determination of the position of the resonance, we calculate the centroid of the correlation function after correcting it from its average and bringing it at a high power exponent k. We use k=10. This operation conveniently limits the less desired tail contribution of the profile in our determination.
The corresponding correlation function C' is given by equation (2):

$$C'^{k} = (C - \langle C^2 \rangle)^k \qquad (2)$$

The spatial shift of the track profile may be quantified in micropad unit Δm, this value being interpreted to determine an analyte refractive index or a biolayer thickness in the case of biosensing. The induced shift in pixels is given by equation (3) as follows:

$$\Delta j_{sensed} = \sum \Delta j C'^{k}(\Delta j) / \sum C'^{k}(\Delta j) \qquad (3)$$

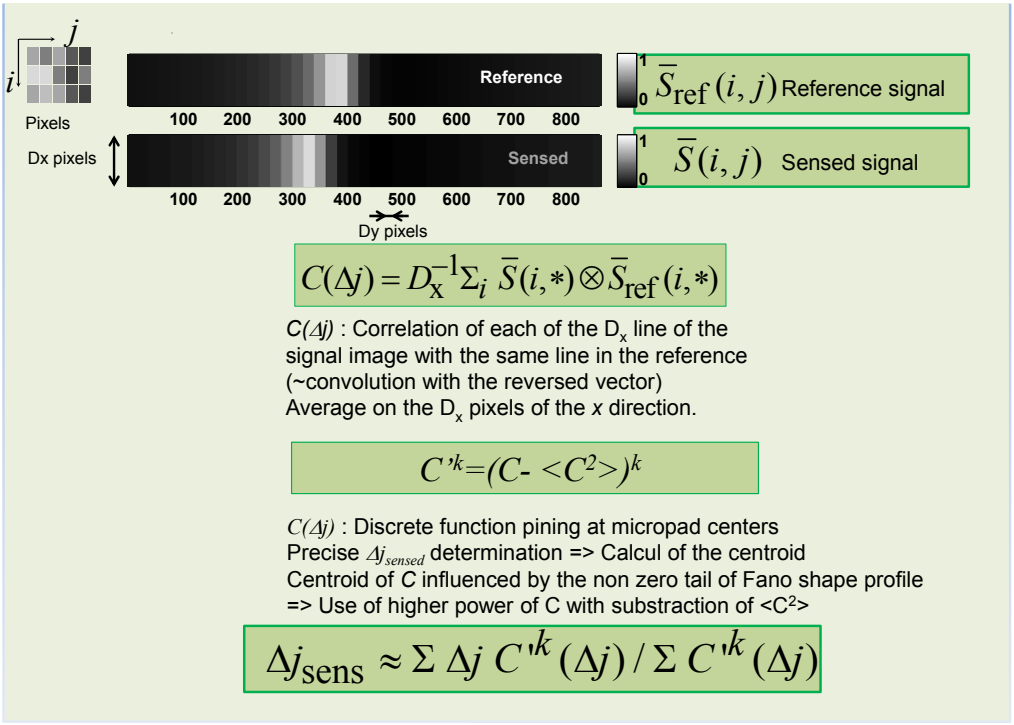

Figure 4: Peak shift calculation determination

Let us stress that this kind of analysis is applicable with any kind of resonant Fano profile, and therefore widely applicable in the field of sensing based on resonant shift. For spectrum, the discretization is usually the number of pixels of the detector, and can be converted in wavelength unit. For angle scan, the discretization samples the angles along the scan.

4. EXPERIMENT

RWG structures are realized by electron-beam lithography. We first choose a glass substrate, and PECVD SiN is then deposited on the substrate, prior to chromium deposition by sputtering [5,9]. The chromium layer serves to reduce charging effect as well as intermediate mask. The resist is then spin-coated prior to electron-beam exposure and development. The chromium can then be etched, followed by the silicon nitride and final removal of the photoresist and chromium layer.

The track images have been measured using a single chip, as illustrated in Figure 5(A), with the wavelength filtered by a monochromator. Measured track images are presented in Figure 5(B). All tracks of this array exhibit a high quality peak-tracking behaviour, with a variation of the underlying Fano parameters from blue to red (the resonance becomes more symmetric on the red side for instance), a trend of the type expected from the constant height step of the grating.

Back to the overall chip design, the chip has 2 set of tracks on its surface, one with 25 tracks to perform sensing over the whole visible range, and one with 3 tracks, serving as reference. Only 3 tracks are made for the reference, in order to save more writing time of the electron-beam lithography process to produce more tracks and longer ones.

The chip is mounted onto a black anodized aluminum holder [10], and the fluid is circulated in a chamber formed by the chip and the holder. This allows to sense small amount of fluid, and is therefore of interest in analytical science or biological analysis applications. It can also be employed for food safety. For instance, we demonstrated the application of the multispectral sensing to oil samples depending on the number of cooking cycle or oil mixture [8].

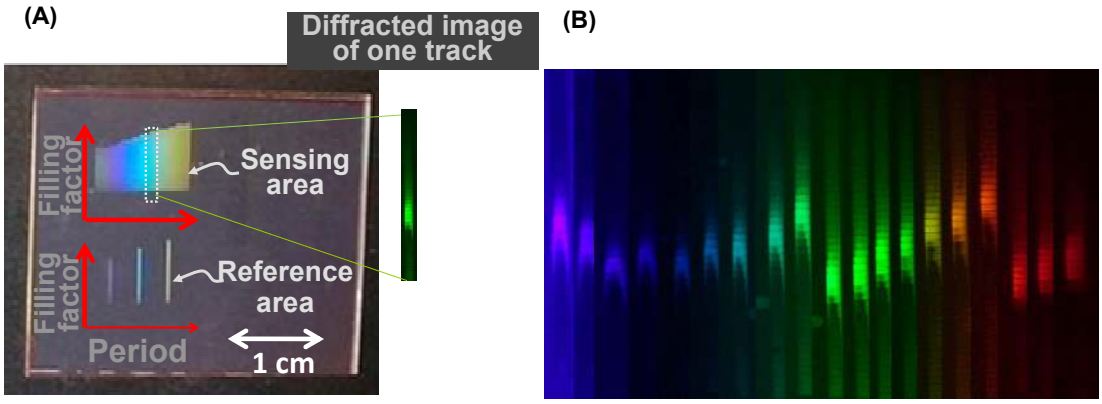

Figure 5: (A) Image of a fabricated chip for multispectral sensing with 25 tracks of varying period (steps of 10 nm) to allow sensing over the whole visible range, and with 3 additional tracks serving as reference. (B) Track images, with each track image being measured at its corresponding resonant wavelength, but under a single incidence angle

5. CONCLUSION

We presented here a technique "plugging" the advantages of RWGs based sensing to simple imaging instrumentation, and its versatility in term of sensing multiple wavelength. For robustness and sequence based measurement, we integrate the profile dimension inside the chip. Both multiplex and sensitivity aspects have been considered, demonstrating here a new method for self-reference refractive index sensing or bioarray imaging. Sensing of multiple wavelength using the same chip support is of interest, specifically to study spectral properties, while keeping the analyte quantity low [8]. The peak position is best determined using image correlation analysis, which demonstrated robustness against Fano lineshape asymmetry. This technique might be extended to other resonance curves analysis. Together with demonstration of highly accurate fits through correlation analysis, our scheme based on a "Peak-tracking chip" demonstrates a new technique for label-free bioarray imaging or refractive index sensing with a simpler imaging set-up that maintains high performance with cheap lenses. Sampling of spectral properties using the same chip support but varying the nanostructuration is highly advantageous in term of robustness and flexibility of the technique. These multispectral aspects extend the applications of our simple 'chip based' sensing principle. Our demonstration was realised in visible, but other domain of wavelength may also be of interest. Indeed, specific fingerprints observed in the infrared might be studied through this technique, using infrared transparent materials [11,12]. Moreover, as additional advantages in comparison to plasmon-based chips (so-called SPR), dual polarisation studies are also possible. This gives our new technique a large potential for sensitive, robust and versatile sensing.

REFERENCES

[1] Ferrie, A.M., Wu, Q., and Fang, Y. "Resonant waveguide grating imager for live cell sensing" Appl. Phys. Lett. 97, 223704 (2010)

[2] Li, P. Y., Lin, B., Gerstenmaier, J., and Cunningham, B. T. "A new method for label-free imaging of biomolecular interactions," Sens. Act. Chem. 99, 6-13 (2004)

[3] George, S., Block, I.D., Jones, S.I., Mathias, P.C., Chaudhery, V., Wu, H.Y., Vuttipittayamongkol, P., Vodkin, L., and Cunningham, B.T., "Label-free prehybridization DNA microarray imaging using photonic crystals for quantitative spot quality analysis," Anal. Chem. 82, 8551-8557 (2010)

[4] Bougot-Robin, K., Reverchon, J-L., Fromant, M., Mugherli, L., Plateau, P. and Benisty, H., "2D label-free imaging of resonant grating biochips in ultraviolet" Optics Express 18, 11472-11482 (2010)

[5] Bougot-Robin, K., Li, S., Zhang, Y., Hsing, I.M., Benisty, H., Wen, W. "Peak Tracking Chip for Label-Free Optical Detection of Bio-Molecular Interaction and Bulk Sensing," The Analyst 137(20), 4785- 4794 (2012)

[6] Bougot-Robin, K., Wen, W., Benisty, H. "Resonant waveguide sensing made robust by on-chip peak tracking through image correlation" Biomedical Optics Express 3(10), 2436-3451(2012)

[7] David, A., Benisty, H., Weisbuch, C. "Fast factorization rule and plane-wave expansion method for two-dimensional photonic crystals with arbitrary hole-shape," Physical Review B 73(7), 075107 (2006)

[8] Bougot-Robin, K., Cao, W., Li, S., Benisty, H., Wen, W. "A multispectral resonant waveguide nanopatterned chip for robust oil quality monitoring" Sensors and Actuators B: Chemical 216, 221-8 (2015)

[9] Hossain, M.N., Justice, J., Lovera, P., McCarthy, B., O'Riordan, A. and Corbett, B., "High aspect ratio nano-fabrication of photonic crystal structures on glass wafers using chrome as hard mask" Nanotechnology 25(35), 355301 (2014)

[10] Bougot-Robin, K., Kodzius, R., Yue, W., Chen, L., Li, S., Zhang, X.X., Benisty, H., Wen, W. "Real time hybridization studies by resonant waveguide gratings using nanopattern imaging for Single Nucleotide Polymorphism detection,". Biomedical microdevices 16(2), 287-99 (2014)

[11] Bhargava, R. "Infrared spectroscopic imaging: the next generation" Applied spectroscopy 66(10),1091-120 (2012)

[12] Kumar, S., Lahlali, R., Liu, X., Karunakaran, C. "Infrared spectroscopy combined with imaging a new developing analytical tool in health and plant science," Applied Spectroscopy Reviews,00-00 (2016)